

# Attenuation of transcriptional bursting in mRNA transport

Li-ping Xiong<sup>1</sup>, Yu-qiang Ma<sup>1</sup> and Lei-han Tang<sup>2</sup>

<sup>1</sup> National Laboratory of Solid State Microstructures, Nanjing University, Nanjing 210093, China

<sup>2</sup> Department of Physics, Hong Kong Baptist University, Kowloon Tong, Hong Kong

E-mail: lhtang@hkbu.edu.hk

**Abstract.** Due to the stochastic nature of biochemical processes, the copy number of any given type of molecule inside a living cell often exhibits large temporal fluctuations. Here, we develop analytic methods to investigate how the noise arising from a bursting input is reshaped by a transport reaction which is either linear or of the Michaelis-Menten type. A slow transport rate smoothes out fluctuations at the output end and minimizes the impact of bursting on the downstream cellular activities. In the context of gene expression in eukaryotic cells, our results indicate that transcriptional bursting can be substantially attenuated by the transport of mRNA from nucleus to cytoplasm. Saturation of the transport mediators or nuclear pores contributes further to the noise reduction. We suggest that the mRNA transport should be taken into account in the interpretation of relevant experimental data on transcriptional bursting.

## 1. Introduction

Molecular binding and chemical modifications underlying intracellular processes are intrinsically stochastic. They give rise to temporal fluctuations and cell-to-cell variations in the number of molecules of any given type, mask genuine signals and responses, and generally contribute to the phenotypic diversity in a population of genetically identical individuals[1, 2]. Various characteristics of such noise have been under intense quantitative study in the past few years [3, 4]. One of the focal points of the discussion is how the noise propagates along a biological pathway. It has been shown that in cases where the dynamics of the upstream molecules is not affected by the downstream processes (e.g., in gene transcription and translation), a “noise addition rule” generally applies, i.e., each process in the pathway contributes to the overall noise strength in a statistically independent fashion[5, 6]. Modifications to this rule in molecular circuits with feedbacks or “detection” capabilities as in signalling have been examined by Tănase-Nicola and his colleagues[7].

In metabolic pathways and other transport processes, however, the upstream molecule is passed on to the downstream pool in a modified form. The conservation of mass and/or number of molecules in the reaction sets new rules on noise propagation. In a recent work, Levine and Hwa considered this problem in the steady state of a metabolic network[8]. Their results show that fluctuations in the number of intermediate metabolites are generally uncorrelated to each other, upstream or downstream along a pathway or across branches. This, of course, does not exclude dynamic correlations which can be quite nontrivial in driven processes[9]. The full dynamic description of stochastic transport through a network is a very challenging task which has not been fully solved even for a linear pathway[10]. A case of interest in the present context is busy input, where the molecules to be transported are produced in batches separated by long silent intervals. Well-known examples of such behavior include the transcriptional and translational bursting[1, 11] and vesicular transport[12]. In eukaryotic gene expression, a large number of mRNAs are produced over a short period of time and followed by a long silent period as a result of the chromatin remodeling. In prokaryotes, burst of protein copy number can occur as the result of short lifetime of an mRNA transcript. Nutrient uptake in endocytosis can also be viewed as a burst event: each endocytic vesicle transports and releases a large number of extracellular molecules to the target site.

In this paper, we examine the attenuation of bursting noise in a two-compartment model with a stochastic transport channel. The model can be viewed as an improvement over the one-compartment model used previously to analyze the mRNA copy number fluctuations in single-molecule experiments carried out by Raj *et al.*[13] on mammalian cell gene expression. The experiments show that the number of mRNA transcripts produced in a single burst event ranges from a few tens to hundreds. It was argued that such large bursts, if unattenuated, could harm the progression of normal cellular activity[14] due to their large perturbations to the cytoplasmic mRNA and protein levels.

A suggestion was made by Raj *et al.* that the latter could be avoided if the overall protein copy number is kept high by a low protein degradation rate. Our analysis here points to a second possibility: a slow nuclear mRNA processing and export process can also attenuate mRNA bursting and minimize its impact on the downstream protein population.

Supporting this view, an earlier kinetic study of mammalian cell mRNA splicing and nuclear transport has shown that the nuclear dwelling (or retention) time of an mRNA molecule can be comparable to its lifetime in the cytoplasm [15]. This is evidenced in the time required to reach the respective steady state levels for the mRNAs residing in the nucleus and in the cytoplasm, which were measured separately in the experiment. Consistent with this observation, both studies also concluded that, on average, about 10-40% of mRNA are retained in the nucleus. In this respect, the one-compartment model of Raj *et al.*, which considers only the total mRNA copy number in a cell, overestimates fluctuations in the actual number of mRNAs in the cytoplasm that participate in the translation process.

To establish a reasonable model, let us first examine the typical fate of a single mRNA: the mRNA is synthesized in bursts at the transcription site and almost simultaneously processed into an mRNA-protein (mRNP) complex[16, 17]; the mRNP complex diffuses inside the nucleus[18, 19, 20], eventually reaches one of the nuclear pores and exits with the help of export mediators[21, 22]; the mRNA degrades in the cytoplasm. Therefore, our model includes three processes: the transcriptional bursting in the nucleus, the mRNA transport, and the mRNA decay in the cytoplasm. We shall assume that the mRNA transport to the cytoplasm is much slower than the diffusion process, so that the spatial inhomogeneity of the mRNA molecules in the two compartments can be ignored[23].

Both linear and nonlinear transport are considered. In linear transport, the export mediators and nuclear pores are abundant as compared to the transported mRNA. Consequently, the export events are independent of each other. Nonlinear transport corresponds to a situation where queuing of nuclear mRNA takes place due to a limited number of transport mediators or nuclear pores. Its mathematical description is identical to that of the Michaelis-Menten (MM) reaction in enzyme kinetics.

The stochastic bursting and transport processes can be described by the chemical master equation governing the time-dependent distribution of mRNA copy numbers in the two compartments. In the case of linear transport, exact expressions for the copy number fluctuations in a steady-state situation are obtained. The MM transport in the weak noise limit can be treated using the linear noise approximation (LNA)[24]. A novel independent burst approximation (IBA) is introduced to treat the MM transport in the strong fluctuations regime. We also perform stochastic simulations to check the accuracy of the analytic expressions.

The main results of our calculation are summarized in Sec. 3. The noise strength of cytoplasmic mRNA is expressed in terms of the average burst size and the ratio of the mean nuclear and cytoplasmic mRNA copy numbers, which are measurable in

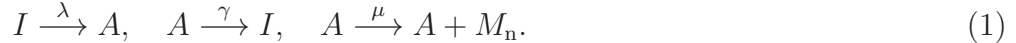
experiments. Quite generally, the extent of burst attenuation is governed by the rate of transport. The slower the mRNA transport, the smaller is the noise in the cytoplasmic mRNA number. In the case of the MM transport, the saturation effect of transport mediators or nuclear pores further reduces mRNA copy number fluctuations in the cytoplasm. Based on these findings, we suggest a revision of the parameters estimated by Raj *et al.* for the bursting and decay dynamics of mRNA in their experiments.

## 2. Methods

The transport event involves two compartments, usually with different volumes which result in different concentrations even when the number of molecules is the same. To step aside this problem and to be more clear, we measure the amount of mRNA in copy number rather than concentration, and define all the reaction rates mesoscopically (by scaling the macroscopic counterparts with volumes). Such a treatment (we will not explicitly refer to specific units for variables and parameters in the following calculations) also facilitates the application of chemical master equations. Then we can start safely by introducing the methods for the simplest case: linear transport.

### 2.1. Linear transport

The burst of mRNA arises from the transitions between active gene  $A$  and inactive gene  $I$ , while each active gene produces an amount of nuclear mRNA  $M_n$ . To faithfully describe the bursting, we write the relevant reactions, as often done in many previous works [1, 13], as:



Here  $\lambda$  and  $\gamma$  are the rates of gene activation and inactivation respectively, and  $\mu$  is the transcription rate. Using  $M_c$  to denote the cytoplasmic mRNA, we define the linear transport and cytoplasmic decay of mRNA as:



Here  $k$  is the transport rate, and  $\delta$  is the degradation rate of cytoplasmic mRNA. The decay of mRNA in nucleus is ignored [15].

At a given time  $t$ , the gene can be in either active or inactive state, with the probabilities given by  $P_A(m_n, m_c, t)$  and  $P_I(m_n, m_c, t)$ , respectively. The probabilities depend on the copy number of mRNA in nucleus  $m_n$  and in cytoplasm  $m_c$ . The time evolution of the two probabilities are governed by the chemical master equations:

$$\begin{aligned} \frac{dP_A(m_n, m_c, t)}{dt} = & \lambda P_I(m_n, m_c, t) - \gamma P_A(m_n, m_c, t) \\ & + \mu(\varepsilon_n^{-1} - 1)P_A(m_n, m_c, t) \\ & + k(\varepsilon_n \varepsilon_c^{-1} - 1)m_n P_A(m_n, m_c, t) \\ & + \delta(\varepsilon_c - 1)m_c P_A(m_n, m_c, t), \end{aligned} \quad (3)$$

$$\begin{aligned} \frac{dP_I(m_n, m_c, t)}{dt} &= \gamma P_A(m_n, m_c, t) - \lambda P_I(m_n, m_c, t) \\ &\quad + k(\varepsilon_n \varepsilon_c^{-1} - 1) m_n P_I(m_n, m_c, t) \\ &\quad + \delta(\varepsilon_c - 1) m_c P_I(m_n, m_c, t), \end{aligned} \quad (4)$$

where  $\varepsilon$  is the step operator defined by its effect on arbitrary functions of  $m_n$  and  $m_c$ :  $\varepsilon_n^{\pm 1} f(m_n, m_c, t) = f(m_n \pm 1, m_c, t)$  and  $\varepsilon_c^{\pm 1} f(m_n, m_c, t) = f(m_n, m_c \pm 1, t)$ .

The first moments or mean values of  $m_n$  and  $m_c$  can be obtained by multiplying equations (3) and (4) by  $m_n$  and  $m_c$  in turn, and summing over all  $m_n$ ,  $m_c$  and gene states:

$$\frac{d\langle m_n \rangle}{dt} = \mu p_A - k\langle m_n \rangle, \quad (5)$$

$$\frac{d\langle m_c \rangle}{dt} = k\langle m_n \rangle - \delta\langle m_c \rangle. \quad (6)$$

Here  $\langle \cdot \rangle$  denotes average over the distribution, and  $p_A(t) \equiv \sum_{m_n, m_c} P_A(m_n, m_c, t)$  is the probability that the gene is in the active state. The following equation is easily seen from the gene activation dynamics (1):

$$dp_A/dt = \lambda(1 - p_A) - \gamma p_A. \quad (7)$$

Equations (5)-(7) are equivalent to the macroscopic rate equations given by the mass-action law due to the linearity of the process. Setting the right-hand-side of these equations to zero, we obtain the steady-state relations for the average mRNA flux:  $J = \mu p_A^* = \mu \lambda / (\lambda + \gamma) = k\langle m_n \rangle = \delta\langle m_c \rangle$ .

In the following discussion we will focus on the burst limit where  $\mu$  and  $\gamma$  are significantly larger than all other reaction rates. The steady-state probability  $p_A^*$  goes to zero but the mRNA synthesis rate  $J = \mu p_A^* \simeq \lambda(\mu/\gamma)$  remains finite. Gene activation in this case follows a Poisson process at a rate  $\lambda$ , but the number of mRNA copies  $b$  produced in each burst event is a random variable that satisfies the geometric distribution:  $G(b) = (\mu/\gamma)^b (1 + \mu/\gamma)^{-b-1}$  [25]. In terms of the mean mRNA copy number produced in each burst,  $\langle b \rangle = \mu/\gamma$ , we have

$$J = \lambda\langle b \rangle = k\langle m_n \rangle = \delta\langle m_c \rangle. \quad (8)$$

A similar procedure as above yields the second moments of mRNA copy numbers in the steady state:

$$\langle m_n^2 \rangle = \langle m_n \rangle^2 + (\langle b \rangle + 1)\langle m_n \rangle, \quad (9)$$

$$\langle m_n m_c \rangle = \langle m_n \rangle \langle m_c \rangle + \langle b \rangle \frac{\langle m_n \rangle \langle m_c \rangle}{\langle m_n \rangle + \langle m_c \rangle}, \quad (10)$$

$$\langle m_c^2 \rangle = \langle m_c \rangle^2 + (\langle b \rangle + 1)\langle m_c \rangle - \langle b \rangle \frac{\langle m_n \rangle \langle m_c \rangle}{\langle m_n \rangle + \langle m_c \rangle}. \quad (11)$$

It is customary to measure temporal variations of population size in a stationary process using the noise strength (also known as the Fano factor), defined as the variance over average [5, 11]:

$$\frac{\sigma_{m_n}^2}{\langle m_n \rangle} = \langle b \rangle + 1, \quad (12)$$

$$\frac{\sigma_{m_c}^2}{\langle m_c \rangle} = \langle b \rangle + 1 - \langle b \rangle \frac{\langle m_n \rangle}{\langle m_n \rangle + \langle m_c \rangle}. \quad (13)$$

For the Poissonian fluctuation arising from the simplest case where molecules are produced one by one with a constant probability and degraded linearly, the noise strength is unity [26, 27]. When the synthesis is burst-like and the degradation is still linear, the noise strength becomes  $\langle b \rangle + 1$ , which is much larger than the Poissonian fluctuation [28]. This is the case for the nuclear mRNA population [equation (12)], and for the mRNA without transport, as in the prokaryotic cells. Equation (13), on the other hand, shows that although the transport event follows a random process, the noise strength of the cytoplasmic mRNA that propagates directly to protein noise, is actually reduced. The amount of reduction is controlled by the ratio  $\langle m_n \rangle / (\langle m_n \rangle + \langle m_c \rangle)$ , which increases with decreasing transport rate  $k$ .

## 2.2. Michaelis-Menten-type transport

Accumulation of the mRNAs in the nucleus may lead to a saturation effect that changes the transport dynamics when the number of export mediators or nuclear pores becomes limiting. This prompts us to study a more general mechanism of transport that takes the transport capacity into account. The resulting process can be cast in the form of the well-known Michaelis-Menten model.

To simplify the discussion, we consider here only one source of constraint, say the limited number of one kind of export mediator denoted by  $E$ , and treat the rest of the export mediators (including the nuclear pores) in the process to be non-rate-limiting. Thus, the transport process of mRNA can be described as:



where  $k_1$  and  $k_2$  are the binding and unbinding rates respectively, and  $k_3$  is the export rate. This is similar to the MM model for enzymatic reaction.

The analysis presented below is based on the ‘‘fast equilibration’’ approximation, in which  $EM_n$  is treated as a transition state rather than an accumulation point in the mRNA export. For this to be true, the lifetime of the complex  $EM_n$  should be significantly shorter than the total nuclear dwelling time, i.e., either the Michaelis constant  $K_m = (k_2 + k_3)/k_1$  is much greater than one, or  $k_3$  is much smaller than the other two rates. Under this assumption, the  $EM_n$  population remains in quasiequilibrium with the nuclear population  $m_n$  which varies on a much slower time scale as compared to the decomposition time of the complex  $EM_n$ .

Due to the small copy number of the nuclear mRNA and the transporter  $E$ , we distinguish the free  $M_n$  from the bound ones, and define the total number of nuclear mRNA as  $m_n = m_{nf} + c$ , where  $m_{nf}$  is the number of free  $M_n$  and  $c$  is the number of the complexes. The total number of  $E$ , including both free and bound ones, is denoted by  $e_t$ . The usual rate equation approach for the complex yields  $k_1 m_{nf} (e_t - c) - (k_2 + k_3)c = 0$

when quasiequilibrium is established. Hence the mean complex number is given by,

$$c = e_t \frac{m_{\text{nf}}}{K_m + m_{\text{nf}}}. \quad (15)$$

On the other hand, through an exact analysis, Levine and Hwa[8] obtained a modified expression in the limit  $k_3 \rightarrow 0$ ,

$$c = e_t \frac{m_n}{K + m_n}, \quad (16)$$

where  $K = K_m + e_t$ . The two expressions converge to the exact result in both the linear regime  $m_n \ll K$  and the saturated regime  $m_n \gg K$ . They differ only in the crossover regime  $m_n \simeq K$ , where no exact result is available in the general case, though either of the two can be used as approximate expressions.

Using equation (16), we write the transport flux as,

$$v(m_n) = k_3 c = \frac{v_{\text{max}} m_n}{K + m_n}, \quad (17)$$

where  $v_{\text{max}} = k_3 e_t$ . Following the fast equilibration assumption, we may now describe the mRNA export under the MM kinetics using the reduced description (2) with an effective transport coefficient  $k = v_{\text{max}}/(K + m_n)$  that decreases with increasing  $m_n$ . Again, taking the burst limit for the mRNA production, we arrive at the following master equation for the joint distribution of  $m_n$  and  $m_c$ :

$$\begin{aligned} \frac{dP(m_n, m_c, t)}{dt} = & \sum_{b=0}^{m_n} \lambda G(b) P(m_n - b, m_c, t) - \sum_{b=0}^{\infty} \lambda G(b) P(m_n, m_c, t) \\ & + (\varepsilon_n \varepsilon_c^{-1} - 1) v(m_n) P(m_n, m_c, t) \\ & + \delta(\varepsilon_c - 1) m_c P(m_n, m_c, t). \end{aligned} \quad (18)$$

Since the nonlinear function  $v(m_n)$  in the MM transport does not allow for the closure of equations for the second moments of the distribution, approximate treatment of the master equation is necessary.

The two limiting situations  $\langle m_n \rangle \gg \langle b \rangle$  and  $\langle m_n \rangle \ll \langle b \rangle$  call for different considerations. In the former case, the contribution of each burst event on the total nuclear mRNA population is small, so that perturbative treatment around the average  $\langle m_n \rangle$  is appropriate. The latter case, however, corresponds to the situation where the nuclear mRNA from each burst event is essentially cleared before the next one arrives. The two cases are treated separately below.

*2.2.1. Linear approximation* We first consider the weak fluctuation case  $\langle m_n \rangle \gg \langle b \rangle$ . A general scheme to perform the noise calculations is the van Kampen's  $\Omega$ -expansion whose lowest order terms reproduce the macroscopic rate equations and the next order terms yield a linear Fokker-Planck equation (FPE), which is often called the linear noise approximation[24]. In Appendix A we derive the noise strengths under the LNA. Here, we outline a more direct yet equivalent way to obtain the results.

The approximation we introduce is to replace (17) with its linear expansion at  $m_n = \langle m_n \rangle$ :

$$v \simeq k_{\text{eff}}(m_n + m_0). \quad (19)$$

Here  $k_{\text{eff}} = v_{\text{max}}K/(K + \langle m_n \rangle)^2$  and  $m_0 = \langle m_n \rangle^2/K$ . Substituting (19) into (18), we may compute moments of the distribution  $P(m_n, m_c, t)$  in the same way as in Sec. 2.1. In fact, equations (8)-(11) remain valid if we make the substitution  $k \rightarrow k_{\text{eff}}$  and  $m_n \rightarrow m_n + m_0$ . After rearranging the terms, we obtain:

$$\frac{\sigma_{m_n}^2}{\langle m_n \rangle} = \left( \frac{\langle m_n \rangle}{K} + 1 \right) (\langle b \rangle + 1), \quad (20)$$

$$\frac{\sigma_{m_c}^2}{\langle m_c \rangle} = \langle b \rangle + 1 - \langle b \rangle \frac{\langle m_n \rangle}{\frac{K\langle m_c \rangle}{K + \langle m_n \rangle} + \langle m_n \rangle}. \quad (21)$$

*2.2.2. Independent burst approximation* In the case  $\langle m_n \rangle \ll \langle b \rangle$ , the mRNA produced in a given burst has sufficient time to exit the nucleus before the next burst arrives. It is then appropriate to consider the independent burst approximation, where individual burst events contribute additively to  $m_n(t)$  and  $m_c(t)$ :

$$m_n(t) = \sum_{t_i < t} \xi(b_i, t - t_i), \quad (22)$$

$$m_c(t) = \sum_{t_i < t} \eta(b_i, t - t_i). \quad (23)$$

Here  $b_i$  is the size of the  $i$ th burst which takes place at  $t_i$ , and  $\xi(b, t)$  and  $\eta(b, t)$  are the number of mRNAs in the nucleus and in the cytoplasm, respectively, generated by a single burst of size  $b$  at  $t = 0$ .

Three independent stochastic processes contribute to the statistical properties of the time series  $m_n(t)$  and  $m_c(t)$ : i) the time of the burst events  $t_i$ , which we assume to be Poisson at a rate  $\lambda$ ; ii) the size  $b_i$  of individual bursts which follow the geometric distribution  $G(b)$ ; and iii) the stochastic nature of the MM transport and mRNA decay in the small copy number regime. In the following discussion we shall focus on the noise effects due to processes i) and ii), while neglecting stochasticity in iii). The latter approximation is justified by noting that the most significant contributions to the quantities computed below are from the period when  $\xi(b, t)$  and  $\eta(b, t)$  are large and their relative fluctuations are small. Denoting by  $x(b, t) = \langle \xi(b, t) \rangle$  and  $y(b, t) = \langle \eta(b, t) \rangle$ , we obtain the following expressions for the moments:

$$\langle m_n \rangle = \sum_b G(b) \int_0^\infty x(b, t) \lambda dt, \quad (24)$$

$$\langle m_n^2 \rangle = \langle m_n \rangle^2 + \sum_b G(b) \int_0^\infty x^2(b, t) \lambda dt, \quad (25)$$

$$\langle m_c \rangle = \sum_b G(b) \int_0^\infty y(b, t) \lambda dt, \quad (26)$$



$$\langle m_c^2 \rangle = \langle m_c \rangle^2 + \sum_b G(b) \int_0^\infty y^2(b, t) \lambda dt, \quad (27)$$

$$\langle m_n m_c \rangle = \langle m_n \rangle \langle m_c \rangle + \sum_b G(b) \int_0^\infty x(b, t) y(b, t) \lambda dt. \quad (28)$$

Under the MM transport (17), the dynamical equations for  $x(b, t)$  and  $y(b, t)$  are given by:

$$\frac{dx}{dt} = -v_{\max} \frac{x}{K+x}, \quad (29)$$

$$\frac{dy}{dt} = v_{\max} \frac{x}{K+x} - \delta y, \quad (30)$$

with the initial condition  $x(b, 0) = b$  and  $y(b, 0) = 0$ .

As shown in Appendix B, the sum and integrals in equations (24) and (25) can be worked out exactly to give:

$$\langle m_n \rangle = \frac{\lambda}{v_{\max}} \langle b \rangle \left( \langle b \rangle + K + \frac{1}{2} \right), \quad (31)$$

$$\sigma_{m_n}^2 \equiv \langle m_n^2 \rangle - \langle m_n \rangle^2 = \frac{\lambda}{v_{\max}} \langle b \rangle \left[ 2\langle b \rangle^2 + (K+2)\langle b \rangle + \frac{K}{2} + \frac{1}{3} \right]. \quad (32)$$

Hence,

$$\frac{\sigma_{m_n}^2}{\langle m_n \rangle} = \langle b \rangle + \frac{1}{2} + \frac{\langle b \rangle^2 + \langle b \rangle + \frac{1}{12}}{K + \frac{1}{2} + \langle b \rangle}. \quad (33)$$

The mean value of  $m_c$  can be obtained from flux balance, i.e.,  $\lambda \langle b \rangle = \delta \langle m_c \rangle$  or  $\langle m_c \rangle = (\lambda/\delta) \langle b \rangle$ . The calculation of  $\langle m_c^2 \rangle$  is a bit more involved which we relegate to Appendix B. Assuming  $\delta \ll v_{\max}$ , i.e., the decay time of an mRNA molecule is much longer than the fastest release time of one mRNA to the cytoplasm, we may write the result in the form:

$$\frac{\sigma_{m_c}^2}{\langle m_c \rangle} = \left( \langle b \rangle + \frac{1}{2} \right) \Psi(u, w), \quad (34)$$

where  $u = \langle b \rangle \delta / v_{\max}$  and  $w = K \delta / v_{\max}$ . The function  $\Psi$  is given by

$$\Psi(u, w) = 2 \int_0^1 dx \int_x^1 dx_1 \frac{e^{w \ln(x/x_1)}}{[1 + u(x_1 - x)]^3}. \quad (35)$$

Since the integrand is less than 1, we have  $\Psi(u, w) \leq 1$ .

We have not managed to find a closed form expression for  $\Psi(u, w)$ , but the integral can be worked out in the two limiting cases: i)  $u = 0$ ,  $\Psi(0, w) = 1/(1+w)$ ; and ii)  $w = 0$ ,  $\Psi(u, 0) = 1/(1+u)$ . These two expressions also set upper bounds for  $\Psi(u, w)$  in general. An approximate expression that is consistent with the two limits and also verified by numerical integration of (35) is given by:

$$\Psi(u, w) \simeq \frac{1}{1+u+w}. \quad (36)$$

In terms of  $\langle m_n \rangle$  and  $\langle m_c \rangle$  and with the help of (31) and the flux balance condition, equation (34) can be rewritten as:

$$\frac{\sigma_{m_c}^2}{\langle m_c \rangle} \simeq \frac{\langle b \rangle + \frac{1}{2}}{1 + \frac{\langle m_n \rangle}{\langle m_c \rangle} \frac{K + \langle b \rangle}{K + \langle b \rangle + \frac{1}{2}}}. \quad (37)$$

### 3. Results and discussion

Let us first summarize the analytical results derived in Section 2 when the average burst size  $\langle b \rangle \gg 1$ . In general, noise strength of mRNA copy number in the two compartments can be expressed in the form,

$$\frac{\sigma_{m_n}^2}{\langle m_n \rangle} = \alpha \langle b \rangle + 1, \quad (38)$$

$$\frac{\sigma_{m_c}^2}{\langle m_c \rangle} = \frac{\langle b \rangle}{1 + \beta \langle m_n \rangle / \langle m_c \rangle} + 1. \quad (39)$$

For the linear model, we have  $\alpha = \beta = 1$ . In the MM case where the transporter may become the bottleneck in the process,  $\alpha = \beta = 1 + \langle m_n \rangle / K$  if the slow transport leads to the nuclear accumulation of mRNA, i.e.,  $\langle m_n \rangle \gg \langle b \rangle$ . In the opposite limit  $\langle m_n \rangle \ll \langle b \rangle$ , where there is nuclear clearance between successive burst events,  $\alpha \simeq 1 + \langle b \rangle / (K + \langle b \rangle)$  and  $\beta \simeq 1$ .

The general trend of noise attenuation on the cytoplasmic mRNA due to delay in nuclear transport is now clear. Retention of the mRNA inside the nucleus decreases the effective burst size and hence the noise strength of the cytoplasmic mRNA. Even at a fixed ratio of  $\langle m_n \rangle$  to  $\langle m_c \rangle$ , further reduction of the noise is possible in the nonlinear MM transport when  $\langle m_n \rangle$  is greater than both the dissociation constant  $K$  and burst size  $\langle b \rangle$ . On the other hand, the independent burst approximation yields a  $\beta$  value close to one, extending the validity of the linear model when the noise strength of  $m_c$  is considered as a function of the ratio of mean copy numbers  $\langle m_n \rangle / \langle m_c \rangle$ .

Fluctuations in the nuclear mRNA level, on the other hand, exhibits a somewhat different behavior. The parameter  $\alpha$  that characterizes the noise strength of  $m_n$  reaches the minimum value 1 in the linear model, but increases when the saturation effect in the MM transport kicks in. Thus queuing results in an enhanced fluctuation upstream of the transport channel.

To check the accuracy of the analytic results under parameter values that broadly correspond to the mammalian cell gene expression experiments mentioned above, we have carried out simulations of the stochastic MM transport defined by (14), following the Gillespie's exact algorithm[29]. The unit of time is chosen such that the mRNA decay rate  $\delta = 1$ . The number of transport channels is set to  $e_t = 10$ . We fix the average mRNA production rate  $\lambda \langle b \rangle$  relative to the mRNA decay rate  $\delta$  such that the mean cytoplasmic mRNA copy number  $\langle m_c \rangle = \lambda \langle b \rangle / \delta = 40$ . For easy comparison with the experimental measurements and analytic results, we also fix the mean nuclear mRNA copy number  $\langle m_n \rangle = 20$ . With these parameter values, the noise strengths in

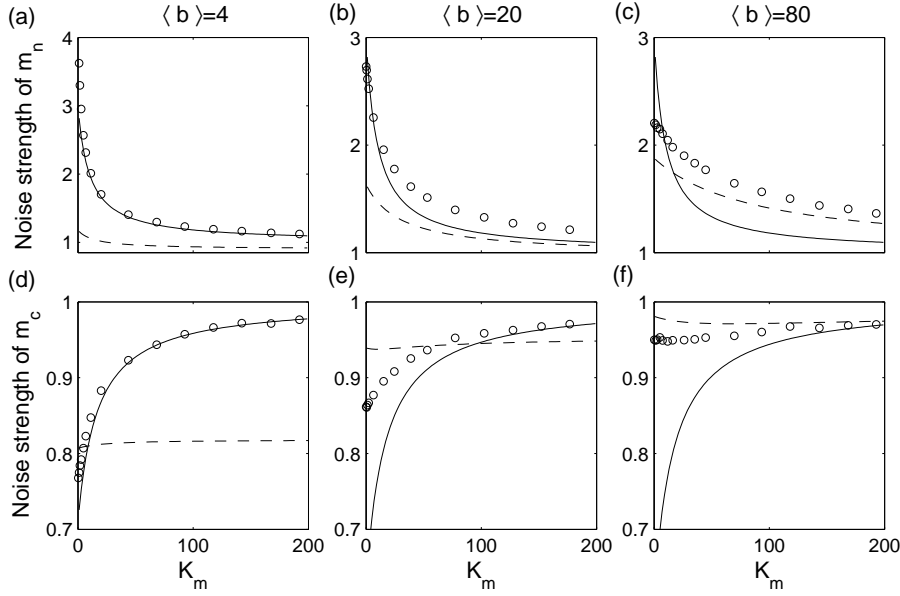


**Figure 1.** Noise strengths (normalized by their corresponding values in the linear model) of the nuclear (upper panel) and the cytoplasmic (lower panel) mRNA copy numbers against the Michaelis constant  $K_m$  which controls saturation of transport channels. Here  $e_t = 10$ ,  $\langle m_n \rangle = 20$  and  $\langle m_c \rangle = 40$ . Results are shown for stochastic simulation (open circles), LNA (solid line) and IBA (dashed line). The overall noise strength is set by the mean burst size  $\langle b \rangle$  which is chosen to be (in units of mRNA copy number): 4 [(a) and (d)]; 20 [(b) and (e)]; 80 [(c) and (f)]. See text for the choice of other model parameters.

the linear model are given by  $\sigma_{m_n}^2 / \langle m_n \rangle = \langle b \rangle + 1$  and  $\sigma_{m_c}^2 / \langle m_c \rangle = \frac{2}{3} \langle b \rangle + 1$ , respectively. Simulations are then performed to examine the effect of channel saturation on the noise strengths by varying the MM parameters  $k_1$  and  $k_3$  in such a way that the mean nuclear mRNA copy number stays at the value set above. The unbinding rate of the mRNA-transporter complex  $EM_n$  is fixed at a low value  $k_2 = 0.1$ .

Figure 1 shows a comparison of simulation data (open circles) and analytic results under the LNA (solid line) and the IBA (dashed line), respectively. Plots on the upper panel give the noise strength of nuclear mRNA as a function of the Michaelis constant  $K_m = (k_2 + k_3)/k_1$ . Fluctuations in  $m_n$  grow as the saturation effect becomes more prominent on the low  $K_m$  side. An opposite trend is seen in the fluctuations of the cytoplasmic mRNA copy number  $m_c$  shown in plots on the lower panel. As expected, the LNA results (solid line) agree well with the simulation data (circles) in the weak burst regime [(a) and (d)], in which case the overall noise strength (as compared to the mean mRNA copy number) is weak. On the other hand, the IBA results (dashed line) represent a better approximation in the strong burst regime [(c) and (f)] [30]. Therefore each of the two approximations perform reasonably well in their respective regimes of validity, and are complementary to each other.

Figure 2 shows the actual distribution [(a) and (c)] and sample time course [(b) and (d)] of the nuclear and cytoplasmic mRNA copy number, respectively, generated from

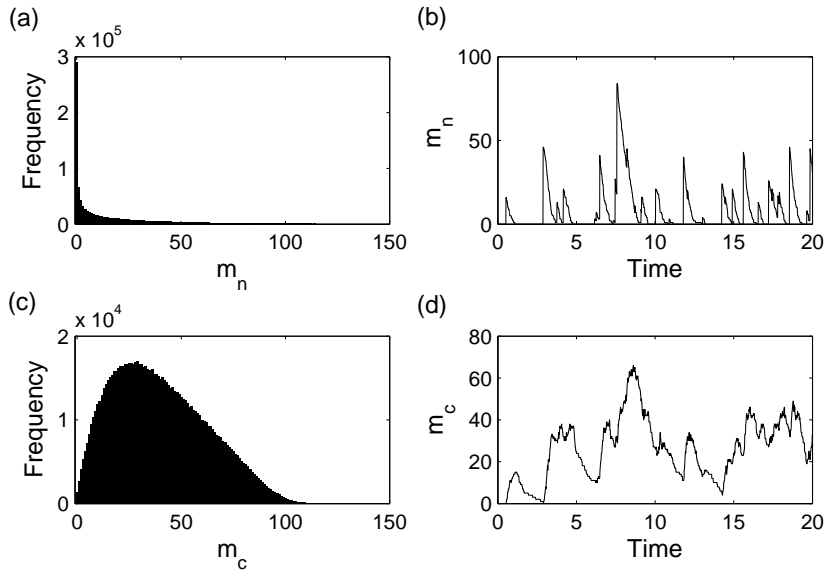


**Figure 2.** Distributions of mRNA copy numbers in the nucleus (a) and in the cytoplasm (c), obtained from 500 000 repeated runs of the Gillespie exact simulation. Sample time courses of  $m_n$  and  $m_c$  in a single simulation are shown in (b) and (d). Parameter values are:  $\lambda = 2$ ,  $\langle b \rangle = 20$ ,  $k_1 = 1.56$ ,  $k_2 = 0.1$ ,  $k_3 = 10$ ,  $e_t = 10$  and  $\delta = 1$ .

simulations at  $K_m = 6.5$ . Other model parameters are the same as that of figure 1 (b) and (e), which represents a borderline case for the two approximate treatments. It is seen from figure 2 (b) that  $m_n$  falls below  $K = 16.5$  most of the time, so approximating the MM transport by a linear expansion at  $m_n = \langle m_n \rangle$  is too crude. On the other hand, there are occasional overlaps of the mRNA produced in successive bursts. This has the effect of slowing down the mRNA transport than what is assumed in the IBA, leading to a somewhat lower  $m_c$  noise as seen in the left part of figure 1 (e).

We have also examined the validity of equation (17) for the mean transport flux. At a given number  $c$  of complexes  $EM_n$ , the expected mRNA export flux is  $k_3 c$ . Therefore  $v(m_n)$  can be obtained in the simulations from the conditional average of  $c$  at a given  $m_n$ . As shown in figure 3, equation (17) (dashed line) fits the simulation data (dots) very well when  $K_m \geq \langle m_n \rangle$  [(c)], but quite poorly in the regime  $K_m \ll \langle m_n \rangle$  [(a)]. Surprisingly, the classic MM equation (15), suitably modified to be considered as a function of  $m_n$ , agrees with the numerical result extremely well for both large and small values of  $K_m$ . Note that equation (17) was derived under the quasi-equilibrium approximation  $k_3 \ll k_1, k_2$  which does not hold in the present case. This inaccuracy may also contribute to the discrepancy between our analytic results and simulation data at small  $K_m$  in figure 1.

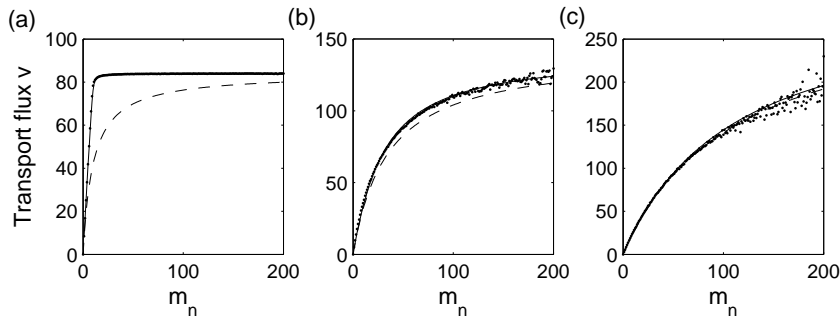


**Figure 3.** Transport flux as calculated from the stochastic simulations (dots), equation (15) (solid line) and equation (17) (dashed line). The transport parameters are: (a)  $k_3 = 8.4$ ,  $K_m = 0.1$ ; (b)  $k_3 = 14$ ,  $K_m = 24.5$ ; (c)  $k_3 = 30$ ,  $K_m = 102.5$ . Other parameter values are given by  $\lambda = 2$ ,  $\langle b \rangle = 20$ ,  $k_2 = 0.1$ ,  $e_t = 10$  and  $\delta = 1$ . Note that  $\langle m_n \rangle = 20$  and  $\langle m_c \rangle = 40$  are the same as before.

#### 4. Conclusions and outlook

The main conclusion of our work is that the nuclear envelope, which sets a natural barrier for the exodus of mature mRNA to the cytoplasm in an eukaryotic cell, can significantly attenuate the effect of transcriptional bursting on the downstream protein population. The extent of the noise reduction on the cytoplasmic mRNA copy number is controlled by the transport efficiency. A high transport rate has a weak effect in noise reduction and essentially brings one back to the one-compartment model considered previously. On the other hand, a low transport rate turns the nucleus into a buffer for the bursting noise, thereby reducing the temporal variation of the mRNA copy number in the cytoplasm. This effect is more dramatic in the saturated regime under the Michaelis-Menten dynamics where, due to the limited availability of transport channels, the mRNA export becomes a Poisson process unaffected by the bursty input.

Our results can be used to re-estimate the mean mRNA burst size in the experiment by Raj and his colleagues. Take the linear transport as an example, the noise strength of the total mRNA copy number in the cell can be obtained from equations (9), (10) and (11):

$$\frac{\sigma_{m_n+m_c}^2}{\langle m_n + m_c \rangle} = \langle b \rangle + 1 + \langle b \rangle \frac{\langle m_n \rangle \langle m_c \rangle}{(\langle m_n \rangle + \langle m_c \rangle)^2}. \quad (40)$$

Thus the average burst size  $\langle b \rangle$  can be obtained from the measured total mRNA fluctuations and the ratio  $\langle m_n \rangle / \langle m_c \rangle$  of nuclear to cytoplasmic mRNA. If 30% of the mRNA accumulate in the nucleus, the burst size should be 83% of that estimated from the model without transport. With the help of the two-compartment models, it would be interesting to revisit the single-molecule experiment data of Raj *et al.* to gain a more complete view of the role of transport on the characteristics of the mRNA noise generated by transcriptional bursting.

Previous studies suggest that for eukaryotes, such as *S. cerevisiae*[1], *Dictyostelium*[31] and mammalian cells[13], transcriptional bursting is a dominant source

of the noise from the internal molecular circuits known as the “internal noise”. It is interesting to note that the stress-related genes, which demand a fast response and an accelerated export rate, are noisier than the essential house-keeping genes such as proteasome genes[32]. In our limited transport capacity model described by the MM dynamics, the downstream noise is indeed stronger in the linear regime and weaker in the saturated regime. The linear regime also allows for a faster response to external stimulus as there is no queuing effect. In this respect, one can not help but wonder whether special processing and export channels are in place in the nucleus for the fast release of stress response genes without congestion.

Finally, we would like to mention that noise propagation through capacity-limited channels with a bursty input is a general phenomenon not limited to the transcriptional bursting, and hence the discussions initiated here can be of broader significance. A somewhat peculiar behavior associated with the limited-capacity transport is that, as the extent of channel saturation increases while maintaining the same average transport current, the noise level of the upstream population increases while that of the downstream population decreases (see figure 1). This counterintuitive phenomenon is neither stochastic resonance (SR) nor stochastic focusing (SF) proposed by Paulsson *et al* [26, 27]. SR is usually related to periodic signal detection, where the signal noise is typically external, while SF exploits signal noise to make a gradual response mechanism work more like a threshold mechanism. Here, the interesting phenomenon we observe is due to a quite different mechanism: the degradation of upstream species and production of downstream species share a common reaction (here transport), whose effective order at steady state can be tuned from zero to one by a combination of reaction parameters.

## Acknowledgments

We thank HG Liu and XQ Shi for helpful discussions. LPX would like to thank the Physics Department, Hong Kong Baptist University for hospitality where part of the work was carried out. This work was supported by the National Natural Science Foundation of China under grant 10629401, and by the Research Grants Council of the HKSAR under grant HKBU 2016/06P.

## Appendix A. The $\Omega$ -expansion

Equations (20) and (21) can be equivalently derived using the more formal  $\Omega$ -expansion which applies when fluctuations of  $m_n$  and  $m_c$  are weak. ( $\Omega$  here stands for the system volume.) To set the notation straight, the rate equation for the copy number  $x_i$  of molecule  $i$  (i.e.,  $m_n$  or  $m_c$  in the present case) is given by,

$$dx_i/dt = \sum_q S_{iq} V_q = (\mathbf{S} \cdot \mathbf{V})_i, \quad (\text{A.1})$$

where  $S_{iq}$  is the stoichiometric coefficient of molecule  $i$  in reaction  $q$ , and  $V_q$  (which depends on the copy numbers in general) is the propensity of reaction  $q$ . Stochasticity

in the problem is assumed to be due to fluctuations in the propensity  $V_q$  with a strength set at  $V_q^{1/2}$  due to the underlying Poisson process.

In the large volume limit and for the steady state, the joint distribution of the  $x_i$ 's, which satisfies the Fokker-Planck equation, can be approximated by a gaussian centered at the solution to the equation  $d\mathbf{x}/dt = \mathbf{S} \cdot \mathbf{V} = 0$ . The width of the distribution is parametrized by a covariance matrix  $\mathbf{C}$  which satisfies the equation [33]:

$$\mathbf{A}\mathbf{C} + \mathbf{C}\mathbf{A}^T + \mathbf{B} = \mathbf{0}. \quad (\text{A.2})$$

Here

$$\mathbf{A}_{ij} = \frac{\partial(\mathbf{S} \cdot \mathbf{V})_i}{\partial x_j}, \quad (\text{A.3})$$

$$\mathbf{B}_{ij} = \sum_q V_q S_{iq} S_{jq}, \quad (\text{A.4})$$

all evaluated at the steady state. Specializing on our two-component problem, there are three reactions: the bursting reaction leading to the production of  $m_n$ , the MM transport reaction for nuclear export, and the mRNA decay in the cytoplasm. Simple calculations yield:

$$\mathbf{A} = \begin{pmatrix} -\frac{v_{\max}K}{(K+\langle m_n \rangle)^2} & 0 \\ \frac{v_{\max}K}{(K+\langle m_n \rangle)^2} & -\delta \end{pmatrix}. \quad (\text{A.5})$$

Application of (A.4) yields:

$$\begin{aligned} B_{11} &= \frac{v_{\max}\langle m_n \rangle}{K + \langle m_n \rangle} + \sum_b \lambda G(b)b^2 \\ &= \frac{v_{\max}\langle m_n \rangle}{K + \langle m_n \rangle} + \lambda\langle b^2 \rangle \\ &= 2\lambda(\langle b \rangle + \langle b \rangle^2). \end{aligned} \quad (\text{A.6})$$

In the last step, we have used the flux-balance condition and  $\langle b^2 \rangle = 2\langle b \rangle^2 + \langle b \rangle$ . Other matrix elements of  $\mathbf{B}$  can be obtained as:

$$B_{12} = B_{21} = -\lambda\langle b \rangle, \quad B_{22} = 2\lambda\langle b \rangle. \quad (\text{A.7})$$

Substituting the values of  $\mathbf{A}$  and  $\mathbf{B}$  into equation (A.2) gives:

$$\sigma_{m_n}^2 = C_{11} = \frac{\langle m_n \rangle(\langle m_n \rangle + K)}{K}(\langle b \rangle + 1), \quad (\text{A.8})$$

$$\langle m_n m_c \rangle - \langle m_n \rangle \langle m_c \rangle = C_{12} = C_{21} = \langle b \rangle \frac{\langle m_n \rangle \langle m_c \rangle}{\frac{K\langle m_c \rangle}{K+\langle m_n \rangle} + \langle m_n \rangle}, \quad (\text{A.9})$$

$$\sigma_{m_c}^2 = C_{22} = \langle m_c \rangle(\langle b \rangle + 1) - \langle b \rangle \frac{\langle m_n \rangle \langle m_c \rangle}{\frac{K\langle m_c \rangle}{K+\langle m_n \rangle} + \langle m_n \rangle}, \quad (\text{A.10})$$

from which equations (20) and (21) follow.

## Appendix B. Integrals in the independent burst approximation

A convenient way to carry out the integrals in (24)-(27) is to convert them into integration over  $x$ , which decreases monotonically from its initial value  $b$  to 0 in a single burst event, with the help of (29) and (30). Following this procedure, we may write,

$$\int_0^\infty dt x(b, t) = - \int_0^b \frac{x dx}{dx/dt} = \int_0^b dx \frac{K+x}{v_{\max}} = \frac{1}{v_{\max}} (Kb + \frac{1}{2}b^2). \quad (\text{B.1})$$

$$\begin{aligned} \int_0^\infty dt x^2(b, t) &= - \int_0^b \frac{x^2 dx}{dx/dt} = \int_0^b x dx \frac{K+x}{v_{\max}} \\ &= \frac{1}{v_{\max}} \left( \frac{1}{2} K b^2 + \frac{1}{3} b^3 \right). \end{aligned} \quad (\text{B.2})$$

To perform the averaging over  $b$ , we make use of the following results for the geometric distribution,

$$\begin{aligned} \langle b^2 \rangle &= \langle b \rangle (1 + 2\langle b \rangle), \\ \langle b^3 \rangle &= \langle b \rangle (1 + 6\langle b \rangle + 6\langle b \rangle^2). \end{aligned}$$

With the help of these results, (31) are (32) are readily obtained.

The dependence of  $y$  on  $x$  follows the equation,

$$\frac{dy}{dx} = \frac{dy/dt}{dx/dt} = -1 + \frac{\delta}{v_{\max}} \left( 1 + \frac{K}{x} \right) y, \quad (\text{B.3})$$

which can be integrated to give,

$$y(x) = \int_x^b dx_1 e^{\delta(x-x_1)/v_{\max} + w \ln(x/x_1)}, \quad (\text{B.4})$$

where  $w \equiv \delta K/v_{\max}$ .

As a check, let us first consider

$$\int_0^\infty dt y = \int_0^b dx \frac{K+x}{v_{\max} x} y. \quad (\text{B.5})$$

Using equation (B.3) and noting that  $y(x=b) = y(x=0) = 0$ , we obtain,

$$\int_0^b dx \frac{K+x}{v_{\max} x} y = \delta^{-1} \int_0^b dx \left( 1 + \frac{dy}{dx} \right) = b/\delta. \quad (\text{B.6})$$

Hence,

$$\langle m_c \rangle = \lambda \langle b \rangle / \delta, \quad (\text{B.7})$$

which is nothing but the conservation law.

We now consider

$$\int_0^\infty dt y^2 = \int_0^b y \delta^{-1} \left( \frac{dy}{dx} + 1 \right) dx = \delta^{-1} \int_0^b y dx. \quad (\text{B.8})$$

Using equation (B.4) and perform the substitution  $x \rightarrow bx$ , we obtain,

$$\int_0^\infty dt y^2 = \frac{b^2}{\delta} \int_0^1 dx \int_x^1 dx_1 e^{b(\delta/v_{\max})(x-x_1) + w \ln(x/x_1)}. \quad (\text{B.9})$$



The averaging over  $b$  can now be readily carried out. Using the result  $\sum_{b=0}^{\infty} b^2 a^b = a(1+a)/(1-a)^3$ , we obtain,

$$\sum_b G(b) \int_0^{\infty} dt y^2(b, t) = \delta^{-1} \int_0^1 dx \int_x^1 dx_1 \frac{e^{w \ln(x/x_1)} a(1+a)}{1 + \langle b \rangle (1-a)^3}. \quad (\text{B.10})$$

Here  $a = \langle b \rangle e^{(x-x_1)\delta/v_{\max}} / (1 + \langle b \rangle)$ .

To avoid run-away accumulation of mRNAs in the nucleus, we require  $\lambda \langle b \rangle < v_{\max}$ . Therefore  $\langle m_c \rangle < v_{\max}/\delta$ . Note that  $\langle m_c \rangle > 1$  automatically implies  $\delta/v_{\max}$  to be a small quantity. In this case, we can approximate  $a \simeq \langle b \rangle [1 + (x - x_1)\delta/v_{\max}] / (1 + \langle b \rangle)$ . Consequently,

$$\sum_b G(b) \int_0^{\infty} dt y^2(b, t) = \frac{\langle b \rangle (\langle b \rangle + \frac{1}{2})}{\delta} \Psi(u, w), \quad (\text{B.11})$$

where  $u = \langle b \rangle \delta / v_{\max}$  and  $\Psi(u, w)$  is given by (35).

Finally, the integral in equation (28) can be rewritten in the form,

$$\int_0^{\infty} dt x(b, t) y(b, t) = \int_0^b x \delta^{-1} \left( \frac{dy}{dx} + 1 \right) dx = \frac{b^2}{2\delta} - \delta^{-1} \int_0^b y dx. \quad (\text{B.12})$$

Comparing with (B.8) and using (B.11), we obtain,

$$\sum_b G(b) \int_0^{\infty} dt x(b, t) y(b, t) = \frac{\langle b \rangle (\langle b \rangle + \frac{1}{2})}{\delta} [1 - \Psi(u, w)]. \quad (\text{B.13})$$

## References

- [1] Raser J M and O'Shea E K 2004 Control of stochasticity in eukaryotic gene expression *Science* **304** 1811-4
- [2] Maamar H, Raj A and Dubnau D 2007 Noise in gene expression determines cell fate in bacillus subtilis *Science* **317** 526-9
- [3] Becskei A and Serrano L 2000 Engineering stability in gene network by autoregulation *Nature* **405** 590-3
- [4] Thattai M and van Oudenaarden A 2001 Intrinsic noise in gene regulatory networks *Proc. Natl. Acad. Sci. USA* **98** 8614-9
- [5] Paulsson J 2004 Summing up the noise in gene networks *Nature* **427** 415-8
- [6] Pedraza J M and Paulsson J 2008 Effects of molecular memory and bursting on fluctuations in gene expression *Science* **319** 339-43
- [7] Tănase-Nicola S, Warren P B and ten Wolde P R 2006 Signal detection, modularity, and the correlation between extrinsic and intrinsic noise in biochemical networks *Phys. Rev. Lett.* **97** 068102
- [8] Levine E and Hwa T 2007 Stochastic fluctuations in metabolic pathways *Proc. Natl. Acad. Sci. USA* **104** 9221-9
- [9] Kardar M, Parisi G and Zhang Y-C 1986 Dynamic scaling of growing interfaces *Phys. Rev. Lett.* **56** 889-92
- [10] Schütz G M 2000 Exactly Solvable Models for Many-Body Systems Far From Equilibrium, in *Phase Transitions and Critical Phenomena* **19** 1-251, Domb C and Lebowitz J (eds.) (Academic Press, London)
- [11] Kærn M, Elston T C, Blake W J and Collins J J 2005 Stochasticity in gene expression: from theories to phenotypes *Nat. Rev. Genet.* **6** 451-64

- [12] Miaczynska M and Stenmark H 2008 Mechanisms and functions of endocytosis *J Cell Biol.* **180** 7-11
- [13] Raj A, Peskin C S, Tranchina D, Vargas D Y and Tyagi S 2006 Stochastic mRNA Synthesis in Mammalian Cells *PLoS Biol.* **4** e309
- [14] Fraser H B, Hirsh A E, Giaever G, Kumm J and Eisen M B 2004 Noise minimization in eukaryotic gene expression *PLoS Biol.* **2** e137
- [15] Audibert A, Weil D and Dautry F 2002 In vivo kinetics of mRNA splicing and transport in mammalian cells *Mol. Cell Biol.* **22** 6706-18
- [16] Orphanides G and Reinberg D 2002 A unified theory of gene expression *Cell* **108** 439-51
- [17] Dreyfuss G, Kim V N and Kataoka N 2002 Messenger-RNA-binding proteins and the messages they carry *Nat. Rev. Mol. Cell Biol.* **3** 195-205
- [18] Shav-Tal Y, Darzacq X, Shenoy S M, Fusco D, Janicki S M, Spector D L and Singer R H 2004 Dynamics of single mRNPs in nuclei of living cells *Science* **304** 1797-800
- [19] Vargas D Y, Raj A, Marras S A E, Kramer F R and Tyagi S 2005 Mechanism of mRNA transport in the nucleus *Proc. Natl. Acad. Sci. USA* **102** 17008-13
- [20] Gorski S A, Dundr M and Misteli T 2006 The road much traveled: trafficking in the cell nucleus *Curr. Opin. Cell Biol.* **18** 284-90
- [21] Izaurralde E and Adam S 1998 Transport of macromolecules between the nucleus and the cytoplasm *RNA* **4** 351-64
- [22] Cole C N and Scarcelli J J 2006 Transport of messenger RNA from the nucleus to the cytoplasm *Curr. Opin. Cell Biol.* **18** 299-306
- [23] The study by Vargas and colleagues on the diffusion of mRNA particles in the nucleus of Chinese hamster ovary (CHO) cell, the same system used in Ref. [13], obtained a diffusion constant  $D = 0.03 - 0.06 \mu\text{m}^2/\text{sec}$  [19]. Given that the diameter of CHO nucleus is about  $5 \mu\text{m}$ , the time needed for the mRNP complexes to disperse throughout the nucleus is of the order of a few minutes, much shorter than the nuclear dwelling time of several hours.
- [24] Van Kampen N G 1992 *Stochastic processes in physics and chemistry* (North-Holland-Elsevier)
- [25] Sánchez Á and Kondev J 2008 Transcriptional control of noise in gene expression *Proc. Natl. Acad. Sci. USA* **105** 5081-6
- [26] Paulsson J, Berg O G and Ehrenberg M 2000 Stochastic focusing: Fluctuation-enhanced sensitivity of intracellular regulation *Proc. Natl. Acad. Sci. USA* **97** 7148-53
- [27] Paulsson J and Ehrenberg M 2000 Random Signal Fluctuations can Reduce Random Fluctuations in Regulated Components of Chemical Regulatory Networks *Phys. Rev. Lett.* **84** 5447-50
- [28] Ozbudak E M, Thattai M, Kurtser I, Grossman A D and van Oudenaarden A 2002 Regulation of noise in the expression of a single gene *Nature Genet.* **31** 69-73
- [29] Gillespie D T 1977 Exact stochastic simulation of coupled chemical reactions *J. Phys. Chem.* **81** 2340-61
- [30] The dashed lines in the lower panel of figure 1 are obtained by evaluating the integral (35) numerically. Direct application of (37) yields nearly identical results.
- [31] Chubb J R, Trcek T, Shenoy S M and Singer R H 2006 Transcriptional pulsing of a developmental gene *Curr. Biol.* **16** 1018-25
- [32] Bar-Even A, Paulsson J, Maheshri N, Carmi M, O'Shea E, Pilpel Y and Barkai N 2006 Noise in protein expression scales with natural protein abundance *Nat. Genet.* **38** 636-43
- [33] Elf J and Ehrenberg M 2003 Fast evaluation of fluctuations in biochemical networks with the linear noise approximation *Genome Res.* **13** 2475-84